

PRECURSORS OF GAMMA-RAY BURSTS: A CLUE TO THE BURSTER'S NATURE

MAXIM LYUTIKOV

Canadian Institute for Theoretical Astrophysics, Toronto, Ontario, M5S 3H8, Canada

VLADIMIR V. USOV

Department of Condensed Matter Physics, Weizmann Institute, Rehovot 76100, Israel

Draft version October 27, 2018

ABSTRACT

In relativistic strongly magnetized winds outflowing from the fast-rotating compact progenitors of gamma-ray bursts (GRBs) there are three regions where powerful high-frequency emission may be generated: (i) the thermal photosphere, (ii) the region of the internal wind instability and (iii) the region of the wind interaction with an ambient gas. This results in a multicomponent structure of GRBs. The emission from the thermal photosphere may be observed as a weak precursor to the main burst. The precursor should have a blackbody-like spectrum with the mean energy of photons of ~ 1 MeV, and its intensity should be tens to hundreds of times smaller than that of the main GRB emission. Observations of such precursors with future γ -ray missions like GLAST can clarify the nature of bursters.

Subject headings: gamma-rays: bursters - stars: neutron - magnetic fields - radiation mechanisms

1. INTRODUCTION

Detections of absorption and emission features at high redshifts in optical afterglows of GRBs and their host galaxies clearly demonstrate that the GRB sources lie at cosmological distances (e.g., Piran 1999; Vietri 1999). Despite such a great advance, the nature of the GRB sources is still unknown. Several currently popular models posit as the energy-releasing event coalescence of two neutron stars (Blinnikov et al. 1984; Paczyński 1986), the collapse of a massive star (Woosley 1993; Paczyński 1998); or accretion induced collapse of magnetic white dwarfs to neutron stars (Usov 1992; Yi & Blackman 1997; Ruderman, Tao & Kluźniak 2000). In all these models, fast-rotating compact objects like millisecond pulsars with the surface magnetic field of $\sim 10^{15} - 10^{17}$ G may be formed (Usov 1992; Blackman, Yi, & Field 1996; Katz 1997; Kluźniak & Ruderman 1998; Vietri & Stella 1998; Spruit 1999; Wheeler et al. 2000). The rotation of these objects decelerates on a time scale of seconds, and relativistic strongly magnetized winds (RSMWs) are generated (e.g., Usov 1999). These winds are plausible sources of cosmological GRBs. In §2 we discuss radiation from RSMWs. More than 2500 GRBs have been detected by BATSE. The large area detectors of BATSE provided excellent light curves of GRBs. Some properties of the light curves expected for GRBs in this model are considered and compared with available data in §3. Our main results are discussed in §4.

2. RADIATION FROM RSMW

Our proposal applies more generally, but, for the sake of concreteness, we consider millisecond pulsars with extremely strong magnetic fields as the sources of RSMWs. The wind outflowing from a such a pulsar is Poynting flux-dominated, i.e., $\sigma = L_{\pm}/L_p \ll 1$, where $L_p \simeq B_s^2 R^6 \Omega^4 / c^3$ is the pulsar luminosity in the Poynting flux, L_{\pm} is its luminosity in both electron-positron pairs and radiation, $R \simeq 10^6$ cm is the radius of the pulsar and Ω is its angular velocity. For typical parameters, $\Omega \simeq 10^4$ s⁻¹

and $B_s \simeq 10^{16}$ G, we have $L_p \simeq 3 \times 10^{52}$ erg s⁻¹ that is about the luminosities of cosmological γ -ray bursters. The more plausible value of σ is $\sim 0.01 - 0.1$ (Usov 1994).

At $L_p \sim 10^{52}$ erg s⁻¹ and $\sigma \sim 0.01 - 0.1$, the density of electron-positron pairs near the compact object is so high that the optical depth for radiation is as high as $\sim 10^{12}$. In this case, the outflowing plasma and radiation are in thermodynamic equilibrium, and the outflowing hot wind may be completely described by L_{\pm} and the mass-loss rate in baryons, \dot{M} . The values of L_{\pm} , σ and \dot{M} may be estimated from observational data on GRBs (see below).

We identify three possible types of high-frequency emission from RSMWs: (i) thermal radiation from the wind photosphere, (ii) non-thermal radiation generated because of the development of internal wind instabilities (iii) non-thermal radiation produced by the interaction between RSMWs and an ambient plasma (see Fig. 1).

2.1. Thermal radiation from the wind photosphere

During outflow, the wind plasma accelerates and its density decreases. At the wind photosphere, $r \simeq r_{\text{ph}}$, the optical depth for the bulk of thermal photons is ~ 1 , and these photons propagate freely at $r > r_{\text{ph}}$. For a spherical electron-positron wind with $\dot{M} = 0$, the radius of the photosphere and the Lorentz factor of the outflowing plasma at this radius are determined by the condition that the comoving plasma temperature at r_{ph} is $T_0 \simeq 2 \times 10^8$ K and by the law $\Gamma \propto r$ for $r \leq r_{\text{ph}}$ (Paczynski 1990; Usov 1994) :

$$r_{\text{ph}} \simeq 3 \times 10^8 \left(\frac{L_{\pm}}{10^{51} \text{ erg s}^{-1}} \right)^{1/4} \text{ cm}, \quad (1)$$

$$\Gamma_{\text{ph}} \simeq 10^2 \left(\frac{L_{\pm}}{10^{51} \text{ erg s}^{-1}} \right)^{1/4}. \quad (2)$$

The mean energy of observed photons is $\langle \varepsilon_{\gamma} \rangle \simeq 2\Gamma_{\text{ph}} T_0 \sim 1$ MeV.

For an optically thick electron-positron wind, the thermal luminosity of the wind photosphere, L_{ph} , practically coincides with L_{\pm} (Usov 1999).

Presence of baryons in RSMWs may change the above estimates. If the mass-loss rate in baryons is small, $\dot{M} < \dot{M}_1 \simeq 10^{-9}(L_{\pm}/10^{51} \text{ erg s}^{-1})^{3/4} M_{\odot} \text{ s}^{-1}$, then the baryonic loading of the wind is negligible. For larger mass-loss rates, $\dot{M}_1 < \dot{M} < \dot{M}_2$, the following relations are valid, $r_{\text{ph}} \propto \dot{M}/\Gamma_{\text{ph}}^2$ and $\Gamma_{\text{ph}} \propto r_{\text{ph}}$, where $\dot{M}_2 = 0.5 \times 10^{-6}(L_{\pm}/10^{51} \text{ erg s}^{-1})^{3/4} M_{\odot} \text{ s}^{-1}$ (e.g., Paczyński 1990). These relations and equations (1) and (2) yield

$$r_{\text{ph}} \simeq 3 \times 10^8 \left(\frac{\dot{M}}{10^{-9} M_{\odot} \text{ s}^{-1}} \right)^{1/3} \text{ cm}, \quad (3)$$

$$\Gamma_{\text{ph}} \simeq 10^2 \left(\frac{\dot{M}}{10^{-9} M_{\odot} \text{ s}^{-1}} \right)^{1/3}. \quad (4)$$

In this case, the photospheric luminosity is about L_{\pm} , similar to a pure electron-positron wind, $(L_{\pm} - L_{\text{ph}})/L_{\pm} = \dot{M}c^2\Gamma_{\text{ph}}/L_{\pm} \simeq (\dot{M}/\dot{M}_2)^{4/3}$. The baryon loading with $\dot{M}_1 < \dot{M} < \dot{M}_2$ does not change essentially the mean energy of photons radiated from the wind photosphere. This is because $\langle \varepsilon_{\gamma} \rangle \propto T_0\Gamma_{\text{ph}}$ while $T_0 \propto r_{\text{ph}}^{-1}$ and $\Gamma_{\text{ph}} \propto r_{\text{ph}}$.

For even larger mass-loss rates, $\dot{M} > \dot{M}_2$, the baryon loading is very important (Paczynski 1990):

$$r_{\text{ph}} \simeq 3 \times 10^9 \left(\frac{\dot{M}}{\dot{M}_2} \right)^3 \left(\frac{L_{\pm}}{10^{51} \text{ erg s}^{-1}} \right)^{1/4} \text{ cm}, \quad (5)$$

$$\Gamma_{\text{ph}} \simeq \frac{L_{\pm}}{\dot{M}c^2} \simeq 10^3 \left(\frac{\dot{M}}{\dot{M}_2} \right)^{-1} \left(\frac{L_{\pm}}{10^{51} \text{ erg s}^{-1}} \right)^{1/4}, \quad (6)$$

Thus, for $\dot{M} > \dot{M}_2$ the photospheric luminosity and the mean energy of thermal photons decrease rapidly ($\propto \dot{M}^{-8/3}$) with increasing \dot{M} .

2.2. Non-thermal radiation from RSMWs

The main source of energy for non-thermal radiation from RSMWs is the magnetic field energy. RSMWs outflowing from the GRB progenitors should resemble the winds from rotation-powered neutron stars (pulsars) (Coroniti 1990; Melatos & Melrose 1996). They have two main components: helical and striped magnetic fields; the striped component alternates in polarity on a scale length of $\pi(c/\Omega) \sim 10^7 \text{ cm}$. At small distances the magnetic field of the wind is frozen into the plasma. As the plasma flows out, the plasma density decreases in proportion to r^{-2} reaching a radius $r_f \sim 10^{13} - 10^{14} \text{ cm}$ where it becomes less than the critical charge density (Goldreich-Julian density) required for the magnetic field to be frozen. At $r > r_f$ the plasma density is not sufficient to screen displacement currents and the striped component of the wind field is transformed into large-amplitude electromagnetic waves (LAEMWs) due to the development of magneto-parametric instability (Usov 1994). The energy of the LAEMWs is, in turn, transferred almost completely to the electron-positron pairs and then to X-ray and γ -ray photons with the typical energy $\langle \varepsilon_{\gamma} \rangle \sim 1 \text{ MeV}$ (Usov 1994; Blackman et al. 1996; Lyutikov & Blackman 2000).

At $r \gg r_f$, the magnetic field is helical everywhere in the outflowing wind. This wind expands more or less freely up to the distance $r_{\text{dec}} \sim 10^{17} \text{ cm}$ at which deceleration of the wind because of its interaction with an interstellar gas becomes important. It was suggested by Mészáros and Rees (1992) that at this distance an essential part of the wind energy may be radiated in X-rays and γ -rays. This suggestion was recently confirmed by numerical simulations (Smolsky & Usov 1996, 2000; Usov & Smolsky 1998). In these simulations it was shown that at $r \sim r_{\text{dec}}$ in the process of the RSMW – ambient gas interaction a shock-like radiating layer forms ahead of the wind front and about 20% of the wind energy may be transferred to high-energy electrons of this layer and then to high frequency (X-ray and γ -ray) emission.

3. LIGHT CURVES: THEORY MEETS OBSERVATIONS

The fact that in RSMWs there are several radiating regions results in a multicomponent structure of GRBs. Since the radiating regions are at different distances from the wind source, sub-pulses generated at the different regions are shifted in time with respect to each other. The first sub-pulse that may be observed in the light curve of a GRB is radiated from the wind photosphere. This sub-pulse looks like a weak precursor of the bulk emission (c.f. Hansen & Lyutikov (2000)). It is expected that the peak intensity of such a precursors is $\sim 10 - 10^2$ times smaller than that of the remaining emission. The precursor has a blackbody-like spectrum, and its duration is about the characteristic time of deceleration of the neutron star rotation $\tau_{\Omega} \sim 0.1 - 10 \text{ s}$. If the outflow from the millisecond pulsar is non-stationary, the radiation of the precursor may be strongly variable. The time scale of this variability may be as small as $\Delta\tau_{\text{ph}} = r_{\text{ph}}/2\Gamma_{\text{ph}}^2c \sim 10^{-6} \text{ s}$. This value is a few orders of magnitude less than the pulsar period $P = 2\pi/\Omega \sim 10^{-3} \text{ s}$. If the angle ϑ between the rotational and magnetic axes of the pulsar is non-zero, $\vartheta \neq 0$, the density of the outflowing plasma may be modulated with the pulsar period. In this case the precursor radiation may be periodical with the pulsar period. Using equations (5) and (6) we can see that this periodical variability may be observed even if the mass-loss rate in baryons \dot{M} is as high as $\sim 10^{-6} M_{\odot} \text{ s}^{-1}$. Hence, observations of both the spectra of GRB precursors and their short-time variability can test the GRB model.

The second component that may be observed in the light curve of a GRB is generated at the distance $r \simeq r_f \sim 10^{13} - 10^{14} \text{ cm}$ where the striped component of the wind field is transformed into LAEMWs. For its generation it is necessary that ϑ is non-zero. This component has a non-thermal spectrum. The time delay between the precursor and the second component is $\Delta\tau_f \simeq r_f/2c\Gamma_0^2$, where Γ_0 is the Lorentz factor of the outflowing plasma at $r \gg r_{\text{ph}}$. The value of Γ_0 is somewhere between Γ_{ph} and $\Gamma_f \sim 10^3$. Using this and equations (2), (4) and (6), for typical parameters, $L_{\pm} \simeq 10^{50} \text{ erg s}^{-1}$, $B_s \simeq 10^{16} \text{ G}$, $\Omega \simeq 10^4 \text{ s}^{-1}$ and $\dot{M} < 10^{-6} M_{\odot} \text{ s}^{-1}$, the value of $\Delta\tau_f$ is in the range from one millisecond to a few seconds. In the extreme case when $\Delta\tau_f$ is as small as $\sim 10^{-3} \text{ s}$, the precursor and the second component practically coincide and cannot be separated from the main components even for the

shortest GRBs. The duration of the second component is $\tau_2 \simeq \max[\tau_\alpha, \Delta\tau_f]$.

The third component that may be observed in the light curve of a GRB is generated at the distance $r \simeq r_{\text{dec}} \sim 10^{17}$ cm where the outflowing wind with a helical magnetic field decelerates due to its interaction with an interstellar gas. The time delay between the precursor and the third component is $\Delta\tau_{\text{dec}} \simeq r_{\text{dec}}/2c\Gamma_0^2$. Numerically, we have that $\Delta\tau_{\text{dec}}$ is ~ 10 s at $\Gamma_0 \simeq 300$ and ~ 100 s at $\Gamma_0 \simeq 100$.

The GRB light curves expected in our model depend on both the angle ϑ between the rotational and magnetic axes and the angle χ between the rotational axis and the sight light. If ϑ is about $\pi/2$, almost all the energy of the Poynting flux - dominated wind is radiated at the distance $r_f \sim 10^{13} - 10^{14}$ cm and transferred to the second component. In this case, the third component is strongly suppressed. On the contrary, if the rotational and magnetic axes are nearly aligned, the third component strongly dominates in GRB light curves irrespective of the χ value. In this case, only a weak second component may be observed. Such a weak second component may imitate a precursor radiated from the wind photosphere, but its spectrum should be nonthermal. Therefore, the nature of a precursor may be found out only when its spectrum is measured. In general case, when ϑ is somewhere between zero and $\pi/2$, both the second and third components with comparable intensities may be seen in GRB light curves.

In our model, the time delay between the precursor and the second component cannot be much more than the rise time of the second component. Figure 2a shows the light curve of GRB 000508a with a weak precursor that is a plausible candidate to be radiated from the wind photosphere. For this GRB, the bulk of its emission is, most probably, the second component radiated at $r \sim r_f$. In the light curves of many GRBs (GRB970411, GRB910522, GRB991216, GRB 000508a, etc.), weak precursors separated by long ($\sim 10 - 100$ s) background intervals were observed (see Fig. 2b). In this case, the bulk of the GRB emission is naturally to identify with the third component. However, to be sure that a weak first episode in GRB light curves is a precursor radiated from the wind photosphere, it is necessary to make sure that its spectrum is nearly blackbody. This may be done for strongest GRBs in near future with GLAST.

4. DISCUSSION

Time histories of long GRBs often show multiple episodes of emission with the count rate dropping to the background level between adjacent episodes (e.g., Fishman et al. 1994; Fishman & Meegan 1995; Meegan 1998). This is well consistent with the idea that there are several space-separated regions where the radiation of a GRB is produced. For some GRBs, the first episode is rather weak and may be treated as a precursor radiated from the wind photosphere. We expect that the most (if not all) GRBs have weak precursors with blackbody-like spectrum. The peak intensity of a precursor is typically about $10 - 10^2$ times less than that of the remaining GRB emission.

Koshut et al. (1995) estimated that $\sim 3\%$ of the GRBs observed with BATSE exhibit precursor activity. However, their definition of precursor activity differs significantly from ours. Indeed, precursor activity was defined by Koshut et al. (1995) as any case in which the first episode has a lower peak intensity than that of the remaining GRB emission and is separated from the remaining emission by a background interval that is at least as long as the remaining emission. In our model, one of the main observational features of a precursor radiated from the wind photosphere is its blackbody-like spectrum, and it is not necessary for the count rate to drop to a background level at all. Therefore, a weak first episode in the light curve of GRB000508a which is slightly ahead of the remaining emission (see Fig. 2a) is a reasonable candidate to be a precursor in our model while from the definition of Koshut et al. (1995) it follows that GRB000508 has no any precursor activity. However, this does not mean that the fraction of GRBs with already observed precursor activity in our conception is higher than $\sim 3\%$. The reason is that for the main part of GRBs discussed in (Koshut et al. 1995) the first episodes have a peak intensity either comparable or only a few times smaller than that of the remaining emission. Such a first episode is, most probably, the second components generated at $r \sim r_f$ while the remaining emission is the third components generated at $r \sim r_{\text{dec}}$.

We thank Norm Murray for useful comments. V.V.U. is grateful for hospitality of the CITA where some of this work was carried out. This work was supported in part by the MINERVA Foundation, Munich, Germany.

REFERENCES

- Blackman, E. G., Yi, I., & Field, G. B. 1996, *ApJ*, 473, L79
 Blinnikov, S. I., Novikov, I. D., Perevodchikova, T. V., & Polnarev, A. G. 1984, *Sov. Astr. Lett.*, 10, 177
 Coroniti, F. V. 1990, *ApJ*, 349, 538
 Fishman, G. J. et al. 1994, *ApJS*, 92, 229
 Fishman, G. J., & Meegan, C. A. 1995, *ARA&A*, 33, 415
 Hansen, B., & Lyutikov, M. 2000, *astro-ph/0003218*
 Katz, J. 1997, *ApJ*, 490, 633
 Kluźniak, W., & Ruderman, M. 1998, *ApJ*, 505, L113
 Koshut, T. M. et al. 1995, *ApJ*, 452, 145
 Lyutikov, M., & Blackman, E. G. 2000, *MNRAS*, submitted
 Meegan, C. A. 1998, *Adv. Sp. Res.*, 22, 1065
 Melatos, A., & Melrose, D. B. 1996, *MNRAS* 279, 1168
 Mészáros, P., & Rees, M. J. 1992, *ApJ*, 397, 570
 Paczyński, B. 1986, *ApJ*, 308, L43
 Paczyński, B. 1990, *ApJ*, 363, 218
 Paczyński, B. 1998, *ApJ*, 494, L45
 Piran, T. 1999, *Phys. Reports*, 314, 575
 Ruderman, M., Tao, L., & Kluźniak, W. 2000, *astro-ph/0003462*
 Smolsky, M. V., & Usov, V. V. 1996, *ApJ*, 461, 858
 Smolsky, M. V., & Usov, V. V. 2000, *ApJ*, 531, 764
 Spruit, H. C. 1999, *A&A*, 341, L1
 Usov, V. V. 1992, *Nature*, 357, 472
 Usov, V. V. 1994, *MNRAS*, 267, 1035
 Usov, V. V. 1999, *Gamma-Ray Bursts: The First Three Minutes*, eds. J. Poutanen and R. Svensson, *ASP Conference Series*, Vol. 190, p. 153
 Usov, V. V., & Smolsky, M. V. 1998, *Phys. Rev. E*, 57, 2267
 Vietri, M. 1999, *astro-ph/9911523*
 Vietri, M., & Stella, L. 1998, *ApJ*, 507, L45
 Wheeler J.C., Yi I., Höflich P., & Wang L. 2000, *ApJ*, in press
 Woosley, S. E. 1993, *ApJ*, 405, 273
 Yi, I., & Blackman, E. G. 1997, *ApJ*, 482, 383

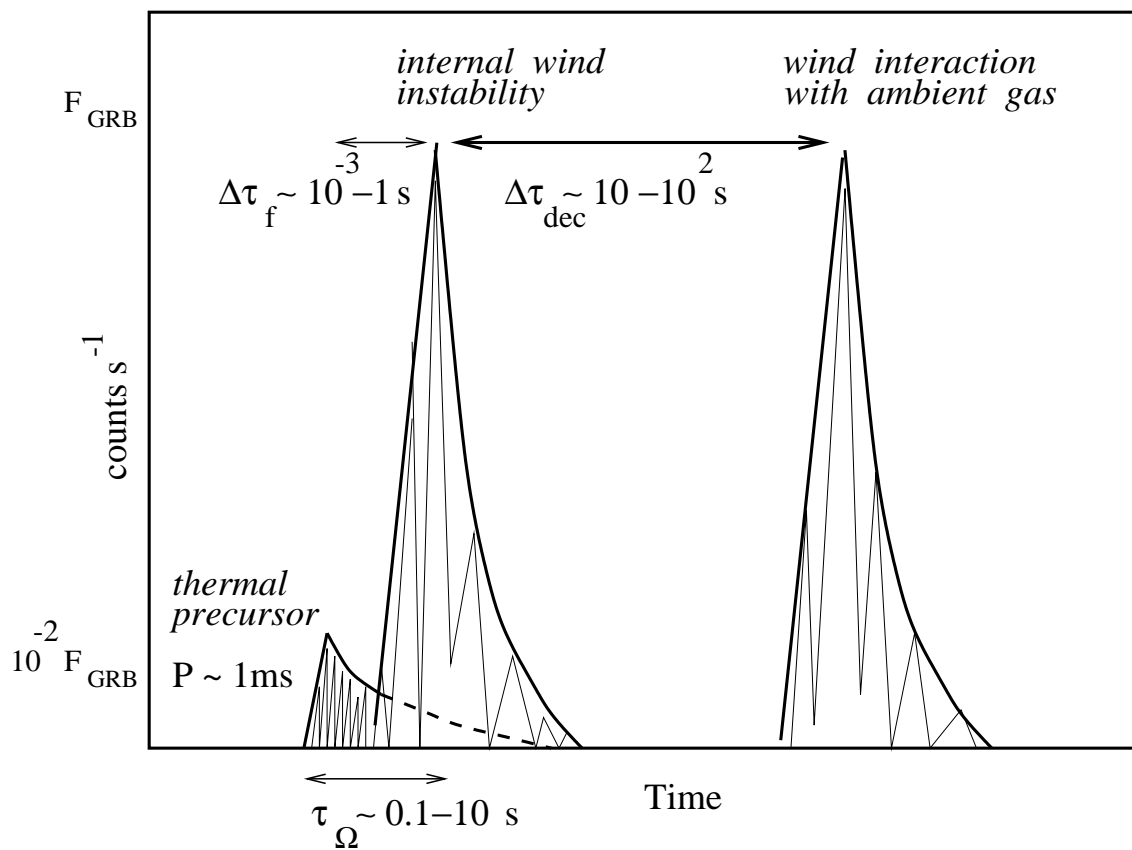


FIG. 1.— Sketch of the light curves expected for GRBs.

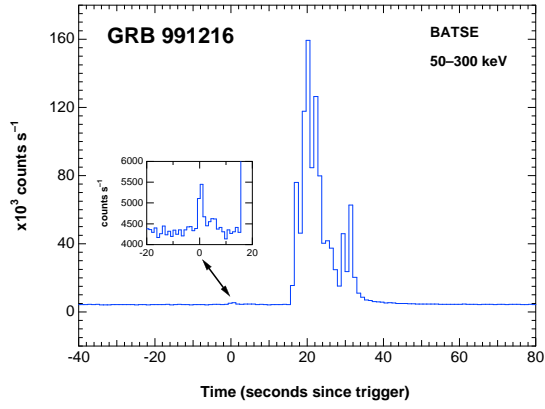
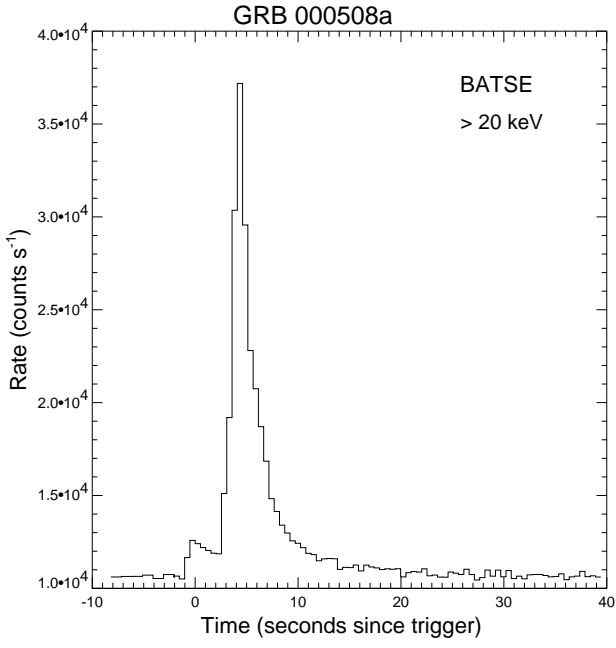


FIG. 2.— Examples of GRBs where precursor may have been observed: (a) GRB 000508, (b) GRB 991216.